Microscopic analysis of the valence transition in tetragonal EuPd₂Si₂

Young-Joon Song¹, Susanne Schulz², Kristin Kliemt³, Cornelius Krellner³, and Roser Valentí¹

Institut für Theoretische Physik, Goethe-Universität Frankfurt,

Max-von-Laue-Straße 1, 60438 Frankfurt am Main, Germany

Institut für Festkörper- und Materialphysik, Technische Universität Dresden, 01062 Dresden, Germany

Kristall- und Materiallabor, Physikalisches Institut, Goethe-Universität Frankfurt,

Max-von-Laue Straße 1, 60438 Frankfurt am Main, Germany

(Dated: February 20, 2023)

Under temperature or pressure tuning, tetragonal $\operatorname{EuPd_2Si_2}$ is known to undergo a valence transition from nearly divalent to nearly trivalent Eu accompanied by a volume reduction. Albeit intensive work, its microscopic origin is still being discussed. Here, we investigate the mechanism of the valence transition under volume compression by *ab initio* density functional theory (DFT) calculations. Our analysis of the electronic and magnetic properties of $\operatorname{EuPd_2Si_2}$ when approaching the valence transition shows an enhanced c-f hybridization between localized Eu 4f states and itinerant conduction states (Eu 5d, Pd 4d, and Si 3p) where an electronic charge redistribution takes place. We observe that the change in the electronic structure is intimately related to the volume reduction where $\operatorname{Eu-Pd}(\operatorname{Si})$ bond lengths shorten and, for the transition to happen, we trace the delicate balance between electronic bandwidth, crystal field splitting, Coulomb repulsion, Hund's coupling and spin-orbit coupling. In a next step we compare and benchmark our DFT results to surface-sensitive photoemission data in which the mixed-valent properties of $\operatorname{EuPd_2Si_2}$ are reflected in a simultaneous observation of divalent and trivalent signals from the Eu 4f shell. The study serves as well to explore the limits of density functional theory and the choice of exchange correlation functionals to describe such a phenomenon as a valence transition.

I. INTRODUCTION

For decades, 4f electron systems have attracted much attention due to the realization of a large variety of interesting phenomena, such as the Kondo effect and the emergence of heavy fermion features, quantum criticality, unconventional superconductivity, exotic magnetism, non-trivial topological phases, or valence transitions, to mention a few [1–8]. Valence transitions have been notably investigated in Eu-based systems where Eu can attain two possible valence states; divalent $\operatorname{Eu}^{2+}(4f^7)$ and trivalent $\operatorname{Eu}^{3+}(4f^6)$. In divalent Eu^{2+} , following the Hund's rule in a LS description, seven electrons fill the f states with a total orbital angular momentum L=0 and a spin momentum $S=\frac{7}{2}$, giving rise to a total angular momentum $J=\frac{7}{2}$. In trivalent Eu^{3+} , L=S=3 and J=0.

Upon lowering the temperature a smooth change of the valency from a non-integer value close to a magnetic $\mathrm{Eu^{2+}}$ state to a non-integer value close to a nonmagnetic $\mathrm{Eu^{3+}}$ state has been observed, for instance, in tetragonal $\mathrm{EuPd_2Si_2}$ [9], $\mathrm{EuCu_2Si_2}$ [10, 11], and $\mathrm{EuIr_2Si_2}$ [12, 13]. Alternatively, such valence transitions were also reported under the application of pressure in tetragonal antiferromagnetic (AFM) $\mathrm{EuRh_2Si_2}$ [14], $\mathrm{EuNi_2Ge_2}$ [15], and $\mathrm{EuCo_2Ge_2}$ [16]. While the valence transition is expected to be related to structural and chemical bonding changes between localized 4f and the more itinerant s, p and d electrons under temperature or pressure effects, a full microscopic description of the transition mechanism is still lacking.

We focus here on the valence transition in $EuPd_2Si_2$ and provide a microscopic analysis of the transition by a

combination of density functional theory (DFT) based calculations and photoemission spectroscopy measurements. We find that, when approaching the valence transition upon volume compression, an enhanced c-f hybridization between localized Eu 4f states and itinerant conduction states (Eu 5d, Pd 4d, and Si 3p) happens where an electronic charge redistribution takes place. We observe that the change in the electronic structure is intimately related to the volume reduction where the Eu-Pd(Si) bond lengths shorten and, for the transition to happen, we trace the delicate balance between electronic bandwidth, crystal field splitting, Coulomb repulsion, Hund's coupling and spin-orbit coupling. The study serves as well to explore the limits of density functional theory and the choice of exchange correlation functionals to describe such a phenomenon as a valence transition.

The paper is organized as follows. In Sec. II we provide a summary of the known properties of EuPd₂Si₂. In Sec. III we describe the methods used for our study. In Sec. IV we present a comparative analysis of structural details in mixed-valence tetragonal Eu compounds Eu TM_2X_2 where TM denotes the transition metal ion and $X=\mathrm{Si}$, Ge. In Sec. V we present our results on the electronic properties of EuPd₂Si₂ for bulk and slab calculations and compare to experimental photoemission measurements. Finally, in Sec. VI we present our conclusions.

II. $EuPd_2Si_2$

The valence transition in mixed-valence tetragonal $EuPd_2Si_2$ was first reported in 1981 in Ref. [9] where a strong isomer shift in Mössbauer spectroscopy was observed when lowering the temperature from 200 K

to 150 K accompanied by an increase in the Eu average valency [9, 17, 18]. The Curie-Weiss moment of EuPd₂Si₂ at high temperatures was reported to be 8.04 μ_B [19], which is very close to the theoretically calculated value of 7.94 μ_B for the divalent state ($J=\frac{7}{2}$). It was then shown by means of x-ray absorption spectroscopy [20, 21], Mössbauer spectroscopy[21], and photoemission spectroscopy [17] measurements that at a temperature of about 200 K EuPd₂Si₂ enters into a valence crossover regime with the mean Eu valency changing smoothly from 2.3 to 2.8 between 200 and 100 K. Interestingly, within the valence crossover the lattice parameter a=4.24 Å at room temperature reduces below 50 K to a=4.16 Å, whereas c remains unchanged [18, 22, 23] [Fig. 1(a)].

Further, applying high pressure can result in EuPd₂Si₂ being in more mixed-valent states. [24–26]. The authors of Ref. [26] argued that the valence transition in EuPd₂Si₂ would also occur under application of an external pressure of about 2 GPa, when a reduces to about 4.16 Å, which is similar to the value of a in the low-temperature regime; specifically, Serdons et al. measured that the mean 4f valence reached about 2.55 at 2 GPa and saturated to about 2.65 at around 5 GPa. [25] Besides, isostructural and isovalent EuPd₂Ge₂ which has a larger unit cell volume than EuPd₂Si₂ doesn't undergo a valence transition at low temperatures but an AFM transition at $T_{\rm N} \approx 17$ K [5]. Actually, the tunability of the Eu valence state by applying chemical and finite hydrostatic pressure was reported in single crystals of $\operatorname{EuPd}_2(\operatorname{Si}_{1-x}\operatorname{Ge}_x)_2$ [27]. At x=0.2 the long-range AFM order of Eu moments observed below $T_{\rm N} \approx 47~{\rm K}$ is suppressed by the application of the hydrostatic pressure of 0.1 GPa inducing an intermediate valence state in Eu. All these observations point to the important role of the structural changes under temperature or pressure affecting the Eu valency.

III. METHODS

We performed DFT calculations using the fullpotential all-electron codes WIEN2k [29], and FPLO [30, 31. The first code considers a linear augmented plane wave basis to solve the Kohn-Sham equations, while the second is based on a local-orbital minimum basis. The exchange-correlation functional was treated within the local (spin) density approximation [L(S)DA] in both WIEN2k and FPLO codes. Crystal bulk structures of EuPd₂Si₂ were fully relaxed in the tetragonal space group I4/mmm within LDA using the open-core approximation as implemented in FPLO until forces were smaller than 1 meV Å. In this approximation the Eu 4f states are removed from the valence basis and enter the bulk description as core orbitals, while fixing the mean 4f occupancy n to a given value. The value of n was considered in steps of 0.1 from 6 to 7 in our structural relaxation. Among various n values, we present results for n = 6.7 (Eu^{2.3+})

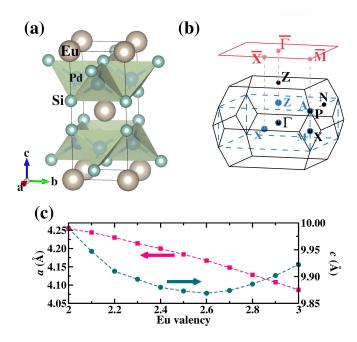


FIG. 1. (a) Crystal structure of tetragonal $\operatorname{EuPd_2Si_2}$, produced by VESTA [28]. (b) First Brillouin zone of the tetragonal I4/mmm (black, solid) and P4/mmm (blue, dashed) structure with special k points for the band structure. The (001) surface was projected in the slab calculations, which is drawn by a pink rectangle. (c) Fully relaxed lattice parameters of $\operatorname{EuPd_2Si_2}$ at each Eu valency obtained using the open-core approximation within LDA.

as an optimized bulk structure at room temperature, and $n = 6.2 \text{ (Eu}^{2.8+})$ as an optimized structure at low temperature (below 30 K), following the suggested mean valencies from the experimental reports in Ref. [9, 17]. The $12\times12\times12$ k-mesh was adopted for atomic position relaxations, while a dense k-mesh of $21 \times 21 \times 21$ was used for accurate total energy calculations to determine the energetically stable structure. All relaxed lattice parameters obtained at each n value in EuPd₂Si₂ are shown in Fig. 1(c), which agree well with the experimentally observed lattice parameters in dependence of the Eu valence states [18, 22, 23]. Specifically, we mention the fully relaxed lattice parameters are a = 4.214 Å and c = 9.895 Åat n = 6.7 (Eu^{2.3+}), and a = 4.128 Å and c = 9.886 Å at n $=6.2 \text{ (Eu}^{2.8+})$. For surface-sensitive electronic structure calculations, we constructed Eu-terminated $1\times1\times4$ slab structures of EuPd₂Si₂ with a vacuum layer of 15 Å using our optimized bulk structure at room temperature and then relaxed the atomic positions of the four layers close to the surface using the *open-core* approximation with n= 6.7 for Eu 4f within LDA in FPLO.

All electronic and magnetic properties were calculated with WIEN2k including spin-orbit coupling (SOC) and correlation effects (U, J_H) so as to deal with the localized nature of Eu 4f orbitals. We fixed U=6 eV and the Hund's coupling $J_H=1$ eV for the Eu atom. The k-mesh sampling was $17\times17\times17$ for the bulk states, and

 $17\times17\times1$ for the slab structure. The size of the basis set was determined by the value of $R_{mt}K_{max}=9.0$ with the muffin-tin radius of 2.5(Eu), 2.4(Pd), 1.95(Si), and 2.25(Ge) in atomic units.

To describe the divalent states (Eu²⁺) in DFT, the inclusion of spin degrees of freedom in spin-polarized calculations was taken into account for simulation purposes, even though EuPd₂Si₂ at room temperature does not magnetically order. We assumed ferromagnetic (FM) spin order with an easy axis parallel to the z-axis. In addition, for the comparison of the electronic structures between EuPd₂Si₂ and EuPd₂Ge₂, an A-type AFM spin order where the Eu magnetic ions are ferromagnetically aligned within the ab plane and antiferromagnetically aligned between consecutive planes was set. The corresponding magnetic space group is P_I4/mnc (No.128.410). For these calculations, we also fully relaxed the EuPd₂Ge₂ crystal bulk structures as we did in EuPd₂Si₂. The fully relaxed lattice parameters in EuPd₂Ge₂ at n = 7 are a = 4.344 Å and c = 10.217 Å, which are also in good agreement with the experiment $(a_{exp} = 4.3764 \text{ Å and } c_{exp} = 10.072 \text{ Å})$ [5].

We would like to note that within DFT it is difficult to trace the valence transition in one single calculation due to the required different treatment of non-magnetic $4f^6$ Eu and magnetic $4f^7$ Eu. The way we approach the valence transition in what follows is therefore by investigating first the two limiting valency situations that require within DFT a different type of calculation, and, we then approach the transition from both sides as a function of volume variation, analyzing the changes in the electronic and magnetic properties of EuPd₂Si₂.

Single crystals of $EuPd_2Si_2$ were grown using the Czochralski method according to the procedure described in Ref. [23]. Angular-resolved photoemission measurements (ARPES) on the (001) surface were performed at the 1^3 ARPES instrument at BESSY II [32]. To prepare a clean surface the samples were cleaved *insitu* under ultra-high vacuum conditions at a temperature of 41 K. In the experiment the energy resolution is better than 50 meV, the angular resolution is better than 0.2 deg.

IV. STRUCTURAL DETAILS

EuPd₂Si₂ crystallizes in a tetragonal body-centered ThCr₂Si₂-type [33] structure with space group I4/mmm (No.139) [22]. It consists of layers of edge-sharing PdSi₄ tetrahedra intercalated between Eu planes, as shown in Fig. 1(a). Eu, Pd and Si are at Wyckoff positions 2a, 4d, and 4e ($z_{\rm rel} = 0.3779$ for Eu^{2.3+} and 0.3818 for Eu^{2.8+}) respectively). Similar to Si, Ge in EuPd₂Ge₂ also sits on the 4e site with $z_{\rm rel} = 0.3715$ for Eu²⁺.

The valence transition in EuPd₂Si₂ is accompanied by a volume contraction where the lattice parameter ashrinks from a=4.24 Å at room temperature to a=4.16 Å below 50 K. To study the relation between volume contraction (and corresponding atomic bond-lengths

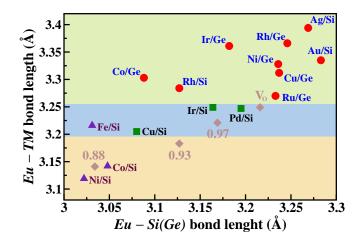


FIG. 2. Classification of tetragonal Eu compounds $EuTM_2X_2$ according to their experimentally reported Eu-TM and Eu-X bond lengths, where TM = Fe, Co, Ni, Cu, Ru, Rh, Pd, Ag, Ir, Au, and X = Si, Ge. Data were obtained from, respectively, TM/X = Ni/Si [34], Co/Si [35], Fe/Si [36], Cu/Si [37], Co/Ge [38], Ir/Si [13], Rh/Si [39], Pd/Si [40], Ir/Ge [41, 42], Ru/Ge [41, 43], Cu/Ge [44, 45], Ni/Ge [36, 38], Rh/Ge [43, 46], Au/Si [47, 48], Ag/Si [47, 49]. Systems with divalent $Eu^{2+\delta}$ states at low temperatures are shown by red circles, whereas purple triangles denote trivalent $\mathrm{Eu}^{3-\delta}$ compounds. Green squares indicate compounds which undergo a valence transition by varying temperature. Brown rhombuses indicate bond lengths of relaxed EuPd₂Si₂ at a given volume with respect to the relaxed one (V_o) calculated for n = 6.7 (see Sec. III). Below $0.93V_0$, bond lengths become similar to those of trivalent Eu compounds.

shortening) with the valence transition, we collected in Fig. 2 crystal information of ThCr₂Si₂-type tetragonal Eu-based compounds $EuTM_2X_2$ whose valence states are confirmed experimentally. Figure 2 illustrates two kinds of bond lengths between Eu and the transition metal (TM) ion, and between Eu and the carbon-group (X) ion, respectively. Red circles indicate tetragonal Eu compounds that show magnetic ground states (e.g., with divalent $\mathrm{Eu}^{2+\delta}$), whereas purple triangles are nonmagnetic ($\mathrm{Eu}^{3-\delta}$) compounds. Systems undergoing a valence transition when temperature decreases are marked by green squares. The following compounds undergo a pressure-induced valence transition at pressures of about 1 GPa for EuRh₂Si₂ [14], 2 GPa for EuNi₂Ge₂ [15], and 3 GPa for EuCo₂Ge₂ [16]. Furthermore, recent surface-sensitive photoemission experiments on tetragonal EuIr₂Si₂, marked by a green square in Fig. 2, reveal divalent Eu²⁺ states in the surface region with twodimensional ferromagnetic order at low temperatures, while in the bulk Eu is almost trivalent and has a nonmagnetic ground state. [50, 51].

Interestingly, EuCu₂Si₂, denoted by a green square in Fig. 2, has been reported to show a valence transition by lowering temperature [10, 11], however, while the authors of Ref. [52] reported the appearance of Eu antiferromagnetism at 10 K in single crystals, the authors of

Ref. [53] suggested that the appearance of volume contractions and corresponding change of Eu valence states at low temperatures originated from the crystallization method and crystal defects. These authors confirmed the presence of trivalent states on a single crystal EuCu₂Si₂ at low temperatures. Actually, the single crystal from Ref. [52] has a larger volume by about 3 % compared to the samples showing trivalent states [53]. Recently, it was found experimentally that bond lengths and valence transition temperature in EuPd₂Si₂ can also change depending on the amount of disorder in the Pd-Si layer [23].

Summarizing the above observations, the Eu valence state in these tetragonal Eu-based compounds is intimately related to the value of Eu-TM and Eu-X bond lengths in the systems. In other words, unlike the previous usual way to refer to systems' volume, the relation between Eu valency and the bond lengths is an interesting parametrization and should be taken into account when it comes to the valence state of Eu on tetragonal Eu-based compounds. In what follows we concentrate on EuPd₂Si₂ and analyze via ab initio DFT the Eu valence transition under volume reduction. It should be noted that in a unit cell volume, there are various atoms involved, and therefore bond lengths and angles may change differently with a given volume change.

V. ELECTRONIC STRUCTURE

A. Calculations for bulk EuPd₂Si₂

We start by examining the description of Eu 4f states in the context of competing Coulomb interaction, crystal field environment, and spin-orbit coupling at ambient pressure. As it is known from atomic physics [54], the description of the electronic structure of an atom depends on the hierarchy of the involved interactions. In the case that the Coulomb interaction between the electrons is stronger than the spin-orbit interactions in each of them, then the total angular momentum $L = \sum_{i} l_{i}$ and total spin $S = \sum_{i} s_{i}$ of the electron system, where l_{i} and s_i are, respectively, the angular momentum and spin of each individual electron, couple to a total J. This situation corresponds to the LS description. If, however, the individual electron coupling via the spin-orbit interaction is stronger than the Coulomb interaction between electrons U_{ee} , then the individual total momenta $j_i = l_i + s_i$, couple to a total $J = \sum_i j_i$ which corresponds to a jj description. Usually the previous description is valid for light atoms, while the second one is more appropriate for heavy atoms. In 4f systems U_{ee} is usually larger than the SOC constant ξ_{SOC} and the LS coupling scheme may be more appropriate [55]. Actually, in a LS description Eu^{2+} $(4f^7)$ has S=7/2, L=0and a total J = 7/2. Alternatively, in the jj description j_i with i = 1, 2, ..., 7 can take values 5/2 and 7/2and the total J in the ground state is then J = 7/2 as well. Analogously Eu^{3+} (4 f^6) in a LS description has

S=L=3 and J=0. Considering the jj description, $j_i,\ i=1,2,...,6$ it results in J=0. The differences between the two schemes is perceived when investigating the magnetic moments [55] $M=g_J\mu_BJ$ where the Landé factor g_J corresponds to the electron gyromagnetic factor $g_J=2$ in the LS scheme, while in the jj coupling $g_J=8/7$ for Eu²⁺. These nuances in the description are important when comparing the calculated magnetic properties to the experiment.

Now we analyze the limiting case of the relaxed structure obtained for n=6.7 (see Sec. III) corresponding to $\mathrm{EuPd_2Si_2}$ at ambient pressure and ambient temperature [17]. Figure 3(a) shows the LSDA + SOC + U calculated electronic structure and corresponding orbital projected densities of states (DOSs) for $\mathrm{EuPd_2Si_2}$ where we assumed a FM configuration for Eu . Due to the half-filled shell $(4f^7)$, the fully occupied 4f bands in the majority spin channel [colored pink in Fig. 3(a)] are centered around -1.0 eV below the Fermi level with a bandwidth of about 1 eV. Note that the energy of the calculated 4f states corresponds to the energy position of the $\mathrm{Eu^{2+}}$ final-state multiplet seen in photoemission, Fig. 5(b).

Furthermore, in this energy range, itinerant conduction states of Pd 4d, Si 3p, and Eu 5d are present, which hybridize with the half-filled Eu 4f bands. Specifically, there is a hole pocket with dominant Eu 5d character at the Γ point, as well as electron pockets with dominant Pd 4d and Si 3p characters at around the X and P points. The calculated total spin moment (M_S) is 6.95 μ_B/Eu with a negligible angular moment of -0.024 μ_B/Eu , which is in good agreement with the values of $S=\frac{7}{2}$ and L=0 expected from the Hund's rule in the divalent Eu^{2+} state in the LS scheme. Specifically, the occupation numbers of each orbital are 6.716 for Eu 4f, 8.016 for Pd 4d, 0.815 for Si 3p, and 0.331 for Eu 5d orbitals. In contrast to EuPd₂Si₂, EuPd₂Ge₂ does not undergo a valence transition at low temperatures but an AFM transition at $T_{\rm N} = 17$ K [5]. This is directly related to the fact that Eu-Pd / Eu-Ge bond lengths in EuPd₂Ge₂ are longer than Eu-Pd / Eu-Si bond lengths in EuPd₂Si₂ and, following Fig. 2, Eu²⁺ states are expected. Our relaxed bond lengths of Eu-Pd / Eu-Ge in EuPd₂Ge₂ differ by 3.2 / 3.9 % from those of Eu-Pd / Eu-Si in EuPd₂Si₂. Figure 3(d) illustrates band structures and Eu 4f orbital projected DOS of A-AFM EuPd₂Si₂ (black) and EuPd₂Ge₂ (cyan) within LSDA + SOC + U. Due to the longer bond lengths, 4f states in EuPd₂Ge₂ near the Fermi level are less dispersive and have a smaller bandwidth than those of EuPd₂Si₂.

We consider now the relaxed EuPd₂Si₂ structure at n=6.2 (see Sec. III). To obtain the electronic structure we performed calculations within LSDA + SOC + U (U=6 eV, $J_{\rm H}=1$ eV), with zero initial magnetization for the Eu atom. Both combined effects, SOC and correlation (U) shift down the occupied sixfold $|j=\frac{5}{2}\rangle$ states to about 6.4 eV below the Fermi level and show almost no dispersion, whereas the empty eightfold $|j=\frac{7}{2}\rangle$ states are located around 1.6 eV above the Fermi level, not shown

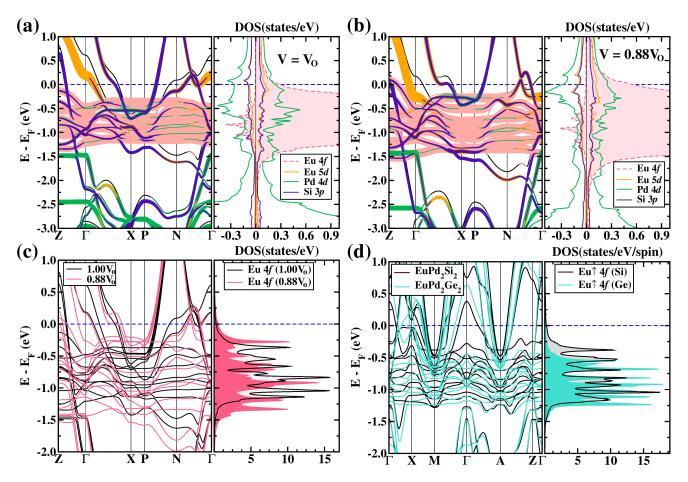


FIG. 3. Fat band electronic structures and orbital projected DOSs obtained from LSDA+SOC+U for (a)-(c) EuPd₂Si₂ and (d) EuPd₂Ge₂. (a) FM band structures for EuPd₂Si₂ at V_o (n=6.7 relaxed structure, see Sec. III) and (b) at a volume of $0.88V_o$. At V_o in (a), the occupied spin-up Eu 4f bands in the FM results are located just below the Fermi level. The energy position of the Eu 4f states is in good agreement with photoemission results, as shown in Fig. 5(b). At $0.88V_o$, the c-f hybridization is enhanced leading to a larger bandwidth of 4f bands in (b). The weight of Eu 4f band characters (a-b) was scaled by a factor of 0.25 for clarity. (c) Overlapped band structures and Eu 4f orbital projected DOSs within LSDA + SOC + U for EuPd₂Si₂ at V_o (black color) and at $0.88V_o$ (light red color). The volume reduction in EuPd₂Si₂ with shorter bond lengths induces an enhanced c-f hybridization leading to more dispersive bands and a larger bandwidth of Eu 4f. (d) Overlapped band structures and orbital projected DOSs for EuPd₂Si₂ (black color) and EuPd₂Ge₂ (cyan color) at V_o both calculated in the A-AFM state. Longer bond lengths in EuPd₂Ge₂ lead to a narrower band width reflecting more localized Eu 4f states compared to EuPd₂Si₂.

here. With the choice of U and $J_{\rm H}$ values above, the energy position of the occupied $|j=\frac{5}{2}\rangle$ states coincides with the position of the trivalent Eu states in photoemission measurements [compare to Fig. 5(b)]. Note, however, that in Fig. 5(b), due to the multiplet nature of trivalent Eu, two separated main peaks are observed at about 7 eV below the Fermi level. This feature is not captured in the DFT calculations, due to the limitations of the method to describe manybody multiplet states.

B. Role of volume reduction on the hybridization

We analyze now the effect of volume reduction on the valence transition from divalent Eu to trivalent Eu in $EuPd_2Si_2$. As mentioned above, this system undergoes

a valence transition by lowering temperature or by increasing pressure $[9,\,26]$. Both effects reduce the volume in EuPd₂Si₂, implying a shortening of the Eu-Pd and Eu-Si bond lengths.

To investigate how the volume reduction affects the electronic structure and the valence state of EuPd₂Si₂, we obtained a few bulk EuPd₂Si₂ structures with a smaller volume than our fully relaxed one (V_o) at n=6.7 by relaxing them using the *open-core* approximation as implemented in FPLO within LDA. Our fully relaxed lattice parameters at n=6.7 (Eu^{2.3+}), which correspond to the room temperature bulk structure at ambient pressure are a=4.214 and c=9.895 Å as given in the Sec. III with bond lengths of Eu-Pd = 3.25 Å and Eu-Si = 3.22 Å. Note that the Eu-Si bond length is in good agreement with our value determined in Ref. [23]. These bond

lengths are marked by a brown rhombus with V_o in Fig. 2. These values are slightly larger than the reported ones in the literature [40]. Also plotted in Fig. 2 are the results for relaxed structures at a volume of $0.97V_o$, $0.93V_o$, and $0.88V_o$. We note that the lattice parameter a for the crystal structure relaxed at $0.97V_o$ is similar to the experimentally reported one at a temperature below 30 K and 0 GPa when the system has undergone the valence transition and has experienced a volume contraction. The values of bond lengths are in the same range as those for compounds that undergo a valence transition (marked by green squares in Fig. 2).

Figure 3(a) and 3(b) show the fat band electronic structure and orbital projected DOSs of FM EuPd₂Si₂ in LSDA+SOC+U at a volume of V_o and $0.88V_o$, respectively. The majority 4f bands are located just below the Fermi level. Compared to the V_o results, at $0.88V_o$ the 4f bandwidth is somewhat larger and more dispersive with an enhanced c-f hybridization. This can be better observed in Fig. 3(c) where we superimposed both electronic structure contributions. Specifically, a reduction of volume leads to a decrease of the occupation number of Eu 4f states, whereas the occupation number in the other orbitals goes up, as shown in Fig. 4 where we display the occupation of Eu 4f, Pd 4d, Si 3p, and Eu 5d states as a function of volume. This is directly related to a shortening of the Eu-TM and Eu-X bond lengths, (see brown rhombuses in Fig. 2) and an enhanced hybridization between Eu 4f and the itinerant conduction states (Eu 5d, Pd 4d, and Si 3p). Further, under volume reduction the total spin moment decreases, whereas the orbital moment increases in magnitude [see Fig. 4(b)]. At $0.88V_o$, the orbital moment of Eu becomes $-0.152 \mu_B/\text{Eu}$ which is a consequence of a slight decrease of the occupation of a mostly $|3,3\rangle$ state, whereas the occupation of the other states remains nearly unchanged. Furthermore, the orbital moment increases to $-0.228 \,\mu_B/\mathrm{Eu}$ at $0.82 V_o$. This behavior shows a tendency to follow the Hund's rules for Eu^{3+} which is L=S=3 and J=|S-L|=0.

We conclude this section by the observation that an LS scheme is more suitable to describe the electronic structure of EuPd₂Si₂ with Eu in the nearly divalent state, while in the case of Eu in a nearly trivalent state corresponding to the reduced volume case, the jj coupling scheme seems more appropriate, as discussed in Ref. [55]. The reason for that is the relative changes in the ratio ξ_{SOC}/U_{ee} [55] where ξ_{SOC} is the spin-orbit coupling strength and U_{ee} the Coulomb interaction. This ratio increases at reduced volumes, as happens while lowering temperature, due to an increased c-f hybridization.

C. Photoemission from the 4f shell

Recently, some of us [50] reported two-dimensional ferromagnetism at a temperature below 48 K in a single Eu layer located below the iridium-silicide surface of tetragonal EuIr₂Si₂, which shows a temperature-driven

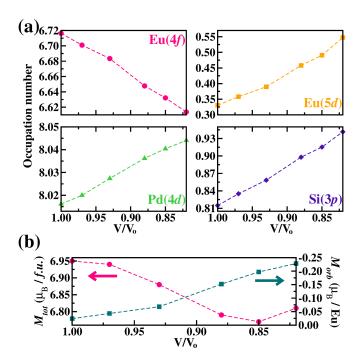


FIG. 4. (a) Occupation number of each orbital as a function of volume reduction of $\mathrm{EuPd_2Si_2}$ within LSDA + SOC + U where V_o corresponds to the structure relaxed with n=6.7 (see Sec. III). When the volume is reduced, the number of occupied Eu 4f states decreases, whereas there is an increase in the other states. (b) Corresponding total spin moment and orbital moment of Eu as a function of volume compression. A decrease of volume results in a decrease of the total spin moment, whereas the orbital moment of Eu increases in magnitude.

valence crossover (marked by a green square in Fig. 2), whereas bulk regions display no magnetism due to the presence of Eu³⁺. In a later experiment, surface ferromagnetism was observed at the Eu-terminated surface of EuIr₂Si₂ as well [51]. Figure 5(b) shows an ARPES spectrum acquired from the (001) surface of a freshly cleaved EuPd₂Si₂ single crystal at a temperature of 41 K. Although the compound was first synthesized decades ago, only recently large single crystals are available [23], enabling ARPES measurements. On the right-hand side of Fig. 5(b) the corresponding angle-integrated spectrum is plotted. To maximally enhance the emission from the 4f shell over contributions from the valence band, we used a photon energy of 145 eV which corresponds to the maximum of the $4d \rightarrow 4f$ Fano-Beutler resonance of Eu^{3+} . Note that at the given photon energy the 4femission of Eu²⁺ is resonantly enhanced as well. In the spectrum, three dominating non-dispersive 4f features are present, which are well established for mixed-valent Eu systems [50, 51, 53, 56] and were reported for photoemission experiments on EuPd₂Si₂, also [57]. Those are (1) the straight line at the Fermi level represents the $4f^7 \rightarrow 4f^6$ final-state multiplet of Eu²⁺ in bulk-like layers; (2) the most intense line at a slightly higher binding

energy of about 1 eV is the surface-core-level shifted 4f emission of $\mathrm{Eu^{2+}}$ at the surface; (3) the broad structure consisting of several lines between 6 and 10 eV forms the $4f^6 \to 4f^5$ final-state multiplet of $\mathrm{Eu^{3+}}$ in bulk-like layers. The simultaneous observation of both the $\mathrm{Eu^{2+}}$ and $\mathrm{Eu^{3+}}$ final-state multiplets reflects the mixed-valent properties of Eu in this compound.

D. Slab calculations

To compare our DFT calculations to the surfacesensitive ARPES measurements presented in the previous section, we constructed a $1\times1\times4$ Eu-terminated slab geometry as described in the Sec. III. Such a geometry allows to disentangle the surface from the bulk states. Due to the symmetric geometry, where the space group of this slab structure is P4/mmm, there are five inequivalent Eu atoms in the unit cell of our slab. Numbering these Eu atoms in relation to proximity to the surface, they are Eu1 through Eu5 with Eu1 at the surface and Eu5 situated furthest from the surface, i.e., located at the center of the unit cell. For the calculation of the electronic structure, we considered FM configurations of these Eu atoms as in our bulk calculations and concentrate therefore on the description of divalent Eu. Figure 5(a) illustrates the (001)-projected band structure and Eu 4f orbital resolved DOS of the slab structure described above for the FM spin configuration in LSDA + SOC + U. All nearly divalent Eu 4f states appear at around 1 eV below the Fermi level. We observe that 4fstates of Eu2, Eu3, Eu4, Eu5 states belonging to the bulk are much closer to the Fermi level than the surface Eu1 states, in agreement with our PES results in the energy range [-3 eV, 0], shown in Fig. 5(b), where a peak from Eu²⁺(surface) is farther from the Fermi level than the weight corresponding to bulk Eu.

VI. CONCLUSIONS

In this work we investigated from first principles the microscopic mechanism of the valence transition in the test-bed system EuPd₂Si₂ which is known to undergo a valence transition from nearly divalent Eu to nearly trivalent Eu upon lowering the temperature. By making use of the observation that the valence transition is accompanied by a volume contraction, we studied the evolution and occurrence of the valence transition by a combination of (i) density functional theory calculations where we considered volume contracted structures, and (ii) photoemission measurements taken at T = 41 K with $h\nu = 145$ eV that were used to benchmark our calculations. Our analysis of the electronic and magnetic properties of EuPd₂Si₂ when approaching the valence transition showed an enhanced c-f hybridization between localized Eu 4f states and itinerant conduction states (Eu 5d, Pd 4d, and Si 3p) where an electronic charge redis-

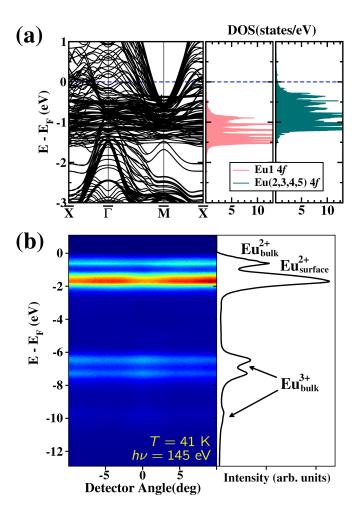


FIG. 5. (a) LSDA + SOC + U electronic band structure and 4f orbital projected DOS of the Eu-terminated $1\times1\times4$ slab structure with a spin configuration where all Eu atoms were set to be of FM order. (b) ARPES spectrum acquired with $h\nu=145~{\rm eV}$ at a temperature of 41 K from the (001) surface of EuPd₂Si₂ for a mixture of Si- and Eu-terminated areas, that shows the Eu 4f emission. On the right, the angle-integrated PES spectrum is given. The DFT calculations capture the distinct surface versus bulk divalent Eu states as observed in the PES experiments in the energy region $[-3~{\rm eV},0]$.

tribution, that we quantified, takes place. The change in the electronic structure was shown to be intimately related to the volume reduction where Eu-Pd(Si) bond lengths shorten. As the bond lengths get shorter the occupation number of the Eu 4f states decreases whereas that of the conduction states increases. For the transition to happen, we observe a delicate balance between electronic bandwidth, crystal field splitting, Coulomb repulsion, Hund's coupling, and spin-orbit coupling that we trace with our calculations.

Further, our DFT EuPd₂Si₂ bulk and Eu-terminated slab results are in good agreement with our surface sensitive photoemission experiments reproducing the presence of divalent Eu states near the Fermi level coming from

surface/bulk Eu and of trivalent Eu states at high binding energies developing from bulk Eu.

With this study we also explored the limits of density functional theory and the choice of exchange correlation functionals to describe such a phenomenon as valence transition.

- [1] S. Wirth and F. Steglich, Exploring heavy fermions from macroscopic to microscopic length scales, Nat. Rev. Mater. 1, 16051 (2016).
- [2] J. G. Rau and M. J. Gingras, Frustrated quantum rare-earth pyrochlores, Annu. Rev. Condens. Matter. Phys. 10, 357 (2019).
- [3] C. Pfleiderer, Superconducting phases of f-electron compounds, Rev. Mod. Phys. 81, 1551 (2009).
- [4] G. R. Stewart, Non-Fermi-liquid behavior in d- and felectron metals, Rev. Mod. Phys. 73, 797 (2001).
- [5] Y. Ōnuki, M. Hedo, and F. Honda, Unique electronic states of Eu-based compounds, J. Phys. Soc. Jpn. 89, 102001 (2020).
- [6] Y. Ōnuki, A. Nakamura, F. Honda, D. Aoki, T. Tekeuchi, M. Nakashima, Y. Amako, H. Harima, K. Matsubayashi, Y. Uwatoko, S. Kayama, T. Kagayama, K. Shimizu, S. Esakki Muthu, D. Braithwaite, B. Salce, H. Shiba, T. Yara, Y. Ashitomi, H. Akamine, K. Tomori, M. Hedo, and T. Nakama, Divalent, trivalent, and heavy fermion states in Eu compounds, Philos. Mag. 97, 3399 (2017).
- [7] Y. Xu, L. Elcoro, Z.-D. Song, B. J. Wieder, M. G. Vergniory, N. Regnault, Y. Chen, C. Felser, and B. A. Bernevig, High-throughput calculations of magnetic topological materials, Nature 586, 702 (2020).
- [8] M. C. Rahn, J.-R. Soh, S. Francoual, L. S. I. Veiga, J. Strempfer, J. Mardegan, D. Y. Yan, Y. F. Guo, Y. G. Shi, and A. T. Boothroyd, Coupling of magnetic order and charge transport in the candidate Dirac semimetal EuCd₂As₂, Phys. Rev. B 97, 214422 (2018).
- [9] E. V. Sampathkumaran, L. C. Gupta, R. Vijayaraghavan, K. V. Gopalakrishnan, R. G. Pillay, and H. G. Devare, A new and unique Eu-based mixed valence system: EuPd₂Si₂, J. Phys. C: Solid State Phys. 14, L237 (1981).
- [10] E. R. Bauminger, D. Froindlich, I. Nowik, S. Ofer, I. Felner, and I. Mayer, Charge Fluctuations in Europium in Metallic EuCu₂Si₂, Phys. Rev. Lett. 30, 1053 (1973).
- [11] S. Patil, R. Nagarajan, C. Godart, J. P. Kappler, L. C. Gupta, B. D. Padalia, and R. Vijayaraghavan, Valence fluctuation in the dilute Eu systems Eu:RPd₂Si₂, Eu:RCu₂Si₂, and Eu:RNiSi₂ (R=La, Y, and Yb), Phys. Rev. B 47, 8794 (1993).
- [12] B. Chevalier, J. M. D. Coey, B. Lloret, and J. Etourneau, EuIr₂Si₂: a new intermediate valence compound, J. Phys. C: Solid State Phys. 19, 4521 (1986).
- [13] S. Seiro, Y. Prots, K. Kummer, H. Rosner, R. Cardoso Gil, and C. Geibel, Charge, lattice and magnetism

VII. ACKNOWLEDGMENTS

We thank Daniel Khomskii, Michael Lang, Igor Mazin and Bernd Wolf for useful discussions. Y.-J. S., K.K., C.K., and R.V. acknowledge support by the Deutsche Forschungsgemeinschaft (DFG, German Research Foundation) for funding through TRR 288 – 422213477 (projects A03, A05). S.S. acknowledges DFG support through Grant No. KR3831/5-1. We thank the Helmholtz-Zentrum Berlin für Materialien und Energie for the allocation of synchrotron radiation beamtime.

- across the valence crossover in EuIr₂Si₂ single crystals, J. Phys.: Condens. Matter **31**, 305602 (2019).
- [14] A. Mitsuda, S. Hamano, N. Araoka, H. Yayama, and H. Wada, Pressure-Induced Valence Transition in Antiferromagnet EuRh₂Si₂, J. Phys. Soc. Jpn. 81, 023709 (2012).
- [15] A. Nakamura, T. Nakama, K. Uchima, N. Arakaki, C. Zukeran, S. Komesu, M. Takeda, Y. Takaesu, D. Nakamura, M. Hedo, K. Yagasaki, and Y. Uwatoko, Effect of pressure on thermopower of EuNi₂Ge₂, J. Phys.: Conf. Ser. 400, 032106 (2012).
- [16] G. Dionicio, H. Wilhelm, Z. Hossain, and C. Geibel, Temperature- and pressure-induced valence transition in EuCo₂Ge₂, Physica B 378-380, 724 (2006).
- [17] K. Mimura, Y. Taguchi, S. Fukuda, A. Mitsuda, J. Sakurai, K. Ichikawa, and O. Aita, Bulk-sensitive high-resolution photoemission study of a temperatureinduced valence transition system EuPd₂Si₂, J. Electron Spectrosc. Relat. Phenom. 137-140, 529 (2004).
- [18] A. Mitsuda, Η. Wada, Μ. Shiga, and Τ. Tanaka, The Euvalence state and ${\rm in}$ $\operatorname{Eu}(\operatorname{Pd}_{1-x}\operatorname{Pt}_x)_2\operatorname{Si}_2$ valence transition J. Phys.: Condens. Matter 12, 5287 (2000).
- [19] A. Mitsuda, H. Wada, M. Shiga, H. Aruga Katori, and T. Goto, Field-induced valence transition of Eu(Pd_{1-x}Pt_x)₂Si₂, Phys. Rev. B 55, 12474 (1997).
- [20] R. Nagarajan, E. Sampathkumaran, L. Gupta, R. Vijayaraghavan, Bhaktdarshan, and B. Padalia, X-ray absorption spectroscopic study of a mixed valence system, EuPd₂Si₂, Phys. Lett. A 81, 397 (1981).
- [21] G. Wortmann, K. Frank, E. Sampathkumaran, B. Perscheid, G. Schmiester, and G. Kaindl, Combined Mössbauer and LIII-edge X-ray absorption study of mixed-valent EuPd₂Si₂ and EuNi₂P₂, J. Magn. Magn. Mater. 49, 325 (1985).
- [22] A. Palenzona, S. Cirafici, and F. Canepa, High Temperature Behaviour of Unstable EuPd₂Si₂ and Reference MPd₂Si₂ Compounds ($M \equiv All$ Rare Earths and Alkaline Earths), J. Less-Common Met. **135**, 185 (1987).
- [23] K. Kliemt, M. Peters, I. Reiser, M. Ocker, F. Walther, D.-M. Tran, E. Cho, M. Merz, A. A. Haghighirad, D. C. Hezel, F. Ritter, and C. Krellner, Influence of the Pd–Si Ratio on the Valence Transition in EuPd₂Si₂ Single Crystals, Cryst. Growth Des. 22, 5399 (2022).
- [24] R. Srinivasan, S. Usha, E. V. Sampathkumaran, and R. Vijayaraghavan, High-pressure magnetic susceptibility of the intermediate valence system EuPd₂Si₂,

- J. Phys. F: Met. Phys. 14, L33 (1984).
- [25] I. Serdons, S. Nasu, R. Callens, R. Coussement, T. Kawakami, J. Ladrière, S. Morimoto, T. Ono, K. Vyvey, T. Yamada, Y. Yoda, and J. Odeurs, Isomer shift determination in Eu compounds using stroboscopic detection of synchrotron radiation, Phys. Rev. B 70, 014109 (2004).
- [26] D. M. Adams, A. E. Heath, H. Jhans, A. Norman, and S. Leonard, The effect of high pressure upon the valence transition in EuPd₂Si₂, J. Phys.: Condens. Matter 3, 5465 (1991).
- [27] B. Wolf, F. Spathelf, J. Zimmermann, T. Lundbeck, M. Peters, K. Kliemt, C. Krellner, and M. Lang, From magnetic order to valence-change crossover in $\text{EuPd}_2(\text{Si}_{1-x}\text{Ge}_x)_2$ using He-gas pressure (2022), arXiv:2210.12227.
- [28] K. Momma and F. Izumi, VESTA 3 for threedimensional visualization of crystal, volumetric and morphology data, J. Appl. Crystallogr. 44, 1272 (2011).
- [29] P. Blaha, K. Schwarz, F. Tran, R. Laskowski, G. K. H. Madsen, and L. D. Marks, WIEN2k: An APW+lo program for calculating the properties of solids, J. Chem. Phys. 152, 074101 (2020).
- [30] K. Koepernik and H. Eschrig, Full-potential nonorthogonal local-orbital minimum-basis band-structure scheme, Phys. Rev. B 59, 1743 (1999).
- [31] I. Opahle, K. Koepernik, and H. Eschrig, Full-potential band-structure calculation of iron pyrite, Phys. Rev. B 60, 14035 (1999).
- [32] S. V. Borisenko, "One-cubed" ARPES User Facility at BESSY II, Synchrotron Radiation News 25, 6 (2012).
- [33] Z. Ban and M. Sikirica, The crystal structure of ternary silicides $\text{Th} M_2 \text{Si}_2(M=\text{Cr},\text{Mn},\text{Fe},\text{Co},\text{Ni}\text{ and Cu}),$ Acta Cryst. **18**, 594 (1965).
- [34] G. Wortmann, I. Nowik, B. Perscheid, G. Kaindl, and I. Felner, Critical evaluation of Eu valences from L_{III} -edge X-ray-absorption and Mössbauer spectroscopy of EuNi₂Si_{2-x}Ge_x, Phys. Rev. B **43**, 5261 (1991).
- [35] P. Maślankiewicz and J. Szade, Valence instability of europium in EuCo₂Si₂, J. Alloys Compd. 423, 69 (2006).
- [36] I. Mayer and I. Felner, Europium silicides and germanides of the $\text{Eu}M_2X_2$ type: Crystal structure and the valence states of europium, J. Phys. Chem. Solids **38**, 1031 (1977).
- [37] A. Palenzona, S. Cirafici, and P. Canepa, High temperature behaviour of the mixed valence compounds $EuCu_2Si_2$, $YbCu_2Si_2$ and the ref- $CaCu_2Si_2$ erence compounds and $GdCu_2Si_2$, J. Less-Common Met. 119, 199 (1986).
- [38] I. Felner and I. Nowik, Magnetism and hyperfine interactions in EuM₂Ge₂ and GdM₂Ge₂(M = Mn, Fe, Co, Ni, Cu), J. Phys. Chem. Solids 39, 767 (1978).
- [39] I. Felner and I. Nowik, Local and itinerant magnetism and superconductivity in RRh₂Si₂ (R = rare earth), Solid State Commun. 47, 831 (1983).
- [40] B. Kuzhel, B. Belan, V. Kuzhel, I. Stets', and R. Serkiz, Contribution of unstable valence states of europium to the electronic transport properties of $\text{EuPd}_{2-x}\text{Si}_{2+x}$, Chem. Met. Alloys **3**, 83 (2010).
- [41] M. Francois, G. Venturini, J. Marêché, B. Malaman, and B. Roques, De nouvelles séries de germaniures, isotypes de U₄Re₇Si₆, ThCr₂Si₂ et CaBe₂Ge₂, dans les systémes ternaires R-T-Ge oú R est un élément des terres rares et T ≡ Ru, Os, Rh, Ir: supraconductivité de LaIr₂Ge₂,

- J. Less-Common Met. 113, 231 (1985).
- [42] A. Prasad, V. K. Anand, Z. Hossain, P. L. Paulose, and C. Geibel, Anisotropic magnetic behavior in EuIr₂Ge₂ single crystal, J. Phys.: Condens. Matter 20, 285217 (2008).
- [43] I. Felner and I. Nowik, Local and itinerant Magnetism AND Crystal structure of RRh₂Ge₂ and RRu₂Ge₂ (r = rare earth), J. Phys. Chem. Solids 46, 681 (1985).
- [44] S. Banik, A. Bendounan, A. Thamizhavel, A. Arya, P. Risterucci, F. Sirotti, A. K. Sinha, S. K. Dhar, and S. K. Deb, Electronic structure of EuCu₂Ge₂ studied by resonant photoemission and x-ray absorption spectroscopy, Phys. Rev. B 86, 085134 (2012).
- [45] W. Iha, T. Yara, Y. Ashitomi, M. Kakihana, T. Takeuchi, F. Honda, A. Nakamura, D. Aoki, J. Gouchi, Y. Uwatoko, T. Kida, T. Tahara, M. Hagiwara, Y. Haga, M. Hedo, T. Nakama, and Y. Ōnuki, Electronic States in EuCu₂(Ge_{1-x}Si_x)₂ Based on the Doniach Phase Diagram, J. Phys. Soc. Jpn. 87, 064706 (2018).
- [46] R. E. Gladyshevskii and E. Parthe, Crystal structure of europium dirhodium digermanium, EuRh₂Ge₂ with ThCr₂Si₂ type, Z. Kristallogr. **198**, 173 (1992).
- [47] I. Mayer, J. Cohen, and I. Felner, The crystal structure of the MAu₂Si₂ rare earth compounds, J. Less-Common Met. 30, 181 (1973).
- [48] M. Abd-Elmeguid, C. Sauer, U. Köbler, W. Zinn, J. Röhler, and K. Keulerz, Valence instability in magnetically ordered $\operatorname{Eu}(\operatorname{Pd}_{1-x}\operatorname{Au}_x)_2\operatorname{Si}_2$, J. Magn. Magn. Mater **47-48**, 417 (1985).
- [49] F. Honda, K. Okauchi, A. Nakamura, D. Aoki, H. Akamine, Y. Ashitomi, M. Hedo, T. Nakama, and Y. Ōnuki, Pressure Evolution of Characteristic Electronic States in EuRh₂Si₂ and EuNi₂Ge₂, J. Phys.: Conf. Ser. 807, 022004 (2017).
- [50] S. Schulz, I. A. Nechaev, M. Güttler, G. Poelchen, A. Generalov, S. Danzenbächer, A. Chikina, S. Seiro, K. Kliemt, A. Y. Vyazovskaya, T. K. Kim, P. Dudin, E. V. Chulkov, C. Laubschat, E. E. Krasovskii, C. Geibel, C. Krellner, K. Kummer, and D. V. Vyalikh, Emerging 2D-ferromagnetism and strong spin-orbit coupling at the surface of valence-fluctuating EuIr₂Si₂, npj Quantum Mater. 4, 26 (2019).
- [51] D. Y. Usachov, A. V. Tarasov, S. Schulz, K. A. Bokai, I. I. Tupitsyn, G. Poelchen, S. Seiro, N. Caroca-Canales, K. Kliemt, M. Mende, K. Kummer, C. Krellner, M. Muntwiler, H. Li, C. Laubschat, C. Geibel, E. V. Chulkov, S. I. Fujimori, and D. V. Vyalikh, Photoelectron diffraction for probing valency and magnetism of 4f-based materials: A view on valence-fluctuating EuIr₂Si₂, Phys. Rev. B 102, 205102 (2020).
- [52] P. G. Pagliuso, J. L. Sarrao, J. D. Thompson, M. F. Hundley, M. S. Sercheli, R. R. Urbano, C. Rettori, Z. Fisk, and S. B. Oseroff, Antiferromagnetic ordering of divalent Eu in EuCu₂Si₂ single crystals, Phys. Rev. B 63, 092406 (2001).
- [53] I. Kawasaki, S.-i. Fujimori, Y. Takeda, H. Yamagami, W. Iha, M. Hedo, T. Nakama, and Y. Ōnuki, Electronic states of EuCu₂Ge₂ and EuCu₂Si₂ studied by soft x-ray photoemission spectroscopy, Phys. Rev. B 100, 035111 (2019).
- [54] G. K. Woodgate, <u>Elementary atomic structure</u>, European physics series (McGraw-Hill, London, New York, 1970).

- [55] T. Hotta, Effect of Spin–Orbit Coupling on Kondo Phenomena in f^7 -Electron Systems, J. Phys. Soc. Jpn. **84**, 114707 (2015).
- [56] I. Kawasaki, M. Kobata, S.-i. Fujimori, Y. Takeda, H. Yamagami, M. Hedo, T. Nakama, and Y. Ōnuki, Electronic structure of the intermediate-valence com-
- pound euni₂p₂ studied by soft x-ray photoemission spectroscopy, Phys. Rev. B **104**, 165124 (2021).
- [57] N. Mårtensson, B. Reihl, W. D. Schneider, V. Murgai, L. C. Gupta, and R. D. Parks, Highly resolved surface shifts in a mixed-valent system: EuPd₂Si₂, Phys. Rev. B 25, 1446 (1982).